A

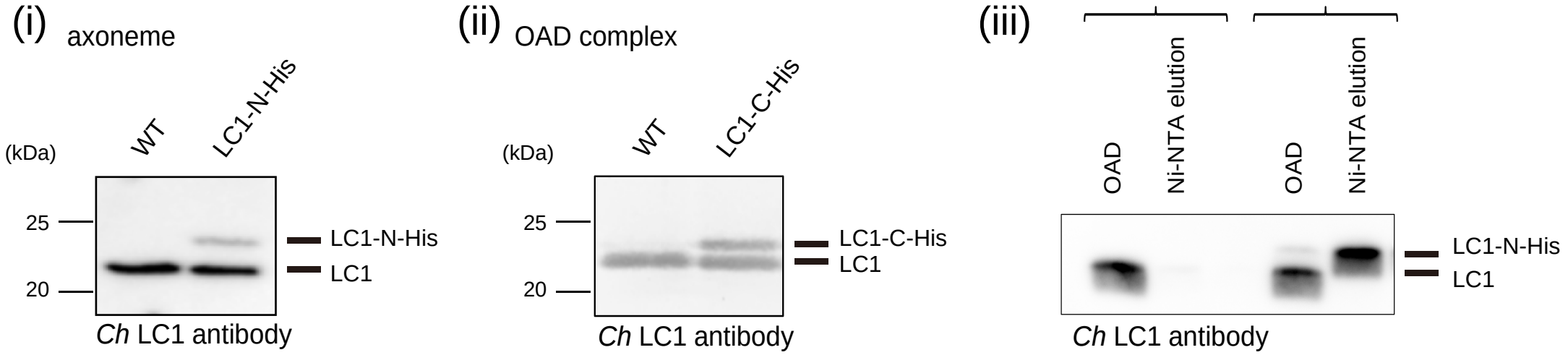
(i) axoneme
WT
LC1-N-His
(kDa)
25
20
LC1-N-His
LC1
Ch LC1 antibody
(ii) OAD complex
WT
LC1-C-His
(kDa)
25
20
LC1-C-His
LC1
Ch LC1 antibody
(iii)
WT
LC1-N-His
OAD
Ni-NTA elution
OAD
Ni-NTA elution
LC1-N-His
LC1
Ch LC1 antibody

B

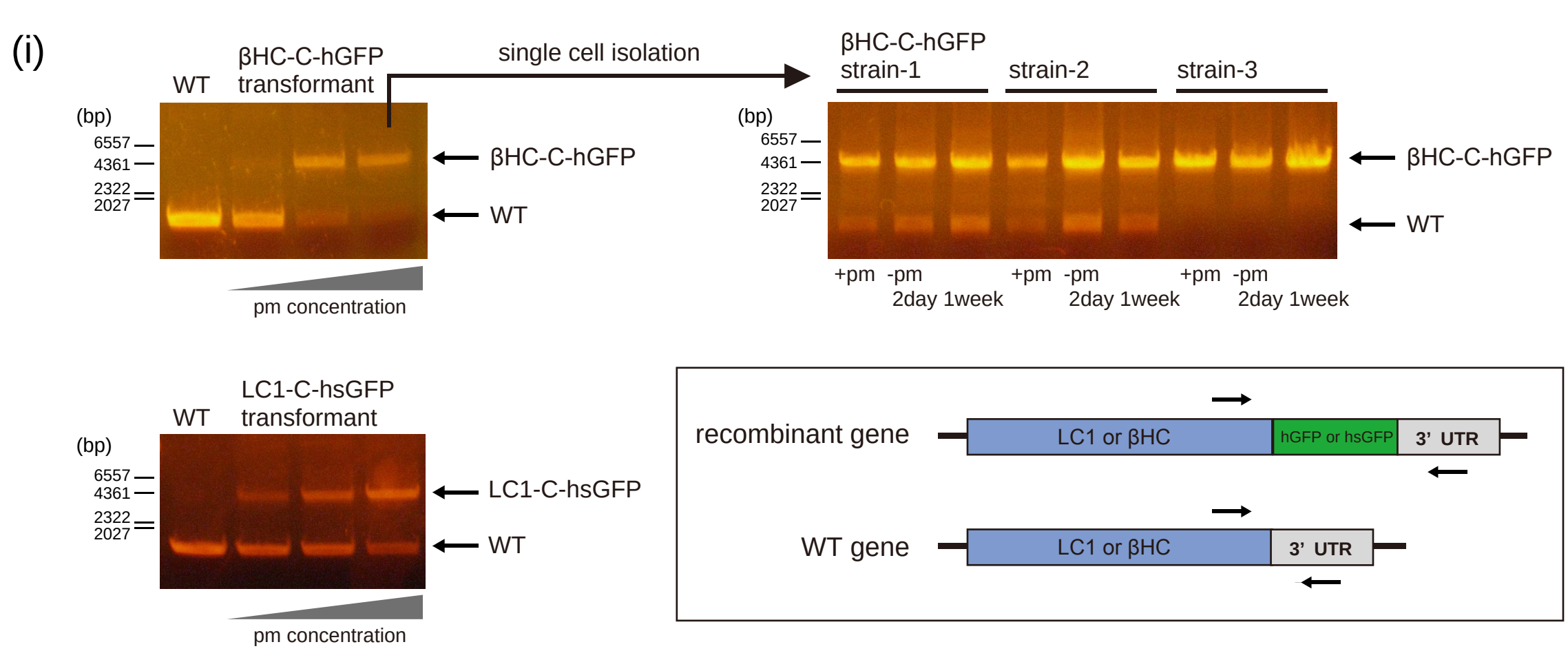
(i)
WT
βHC-C-hGFP transformant
single cell isolation
βHC-C-hGFP strain-1
strain-2
strain-3
(bp)
6557
4361
2322
2027
βHC-C-hGFP
WT
pm concentration
+pm -pm
2day 1week
LC1-C-hsGFP transformant
LC1-C-hsGFP
recombinant gene
LC1 or βHC
hGFP or hsGFP
3' UTR
WT gene
(ii)
βHC-C-hGFP
LC1-C-hsGFP

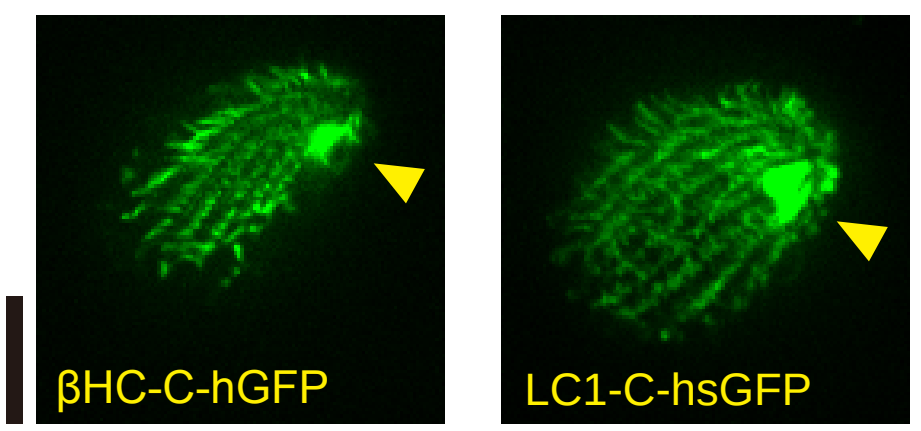
(ii)
βHC-C-hGFP
LC1-C-hsGFP

C

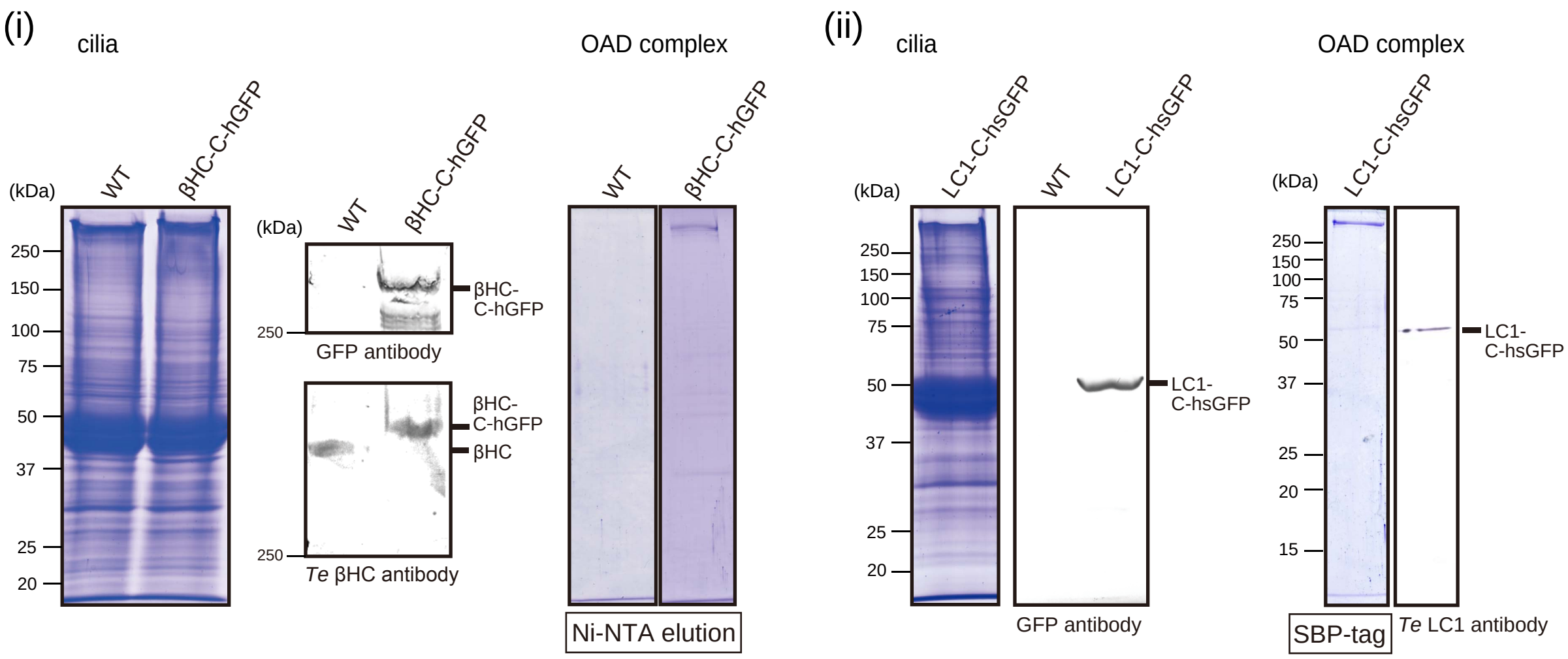
(i)
cilia
OAD complex
WT
βHC-C-hGFP
(kDa)
250
150
100
75
50
37
25
20
GFP antibody
βHC-C-hGFP
Te βHC antibody
βHC
Ni-NTA elution
(ii)
cilia
OAD complex
LC1-C-hsGFP
LC1-C-hsGFP
LC1-C-hsGFP
GFP antibody
SBP-tag
Te LC1 antibody

Fig S1

A

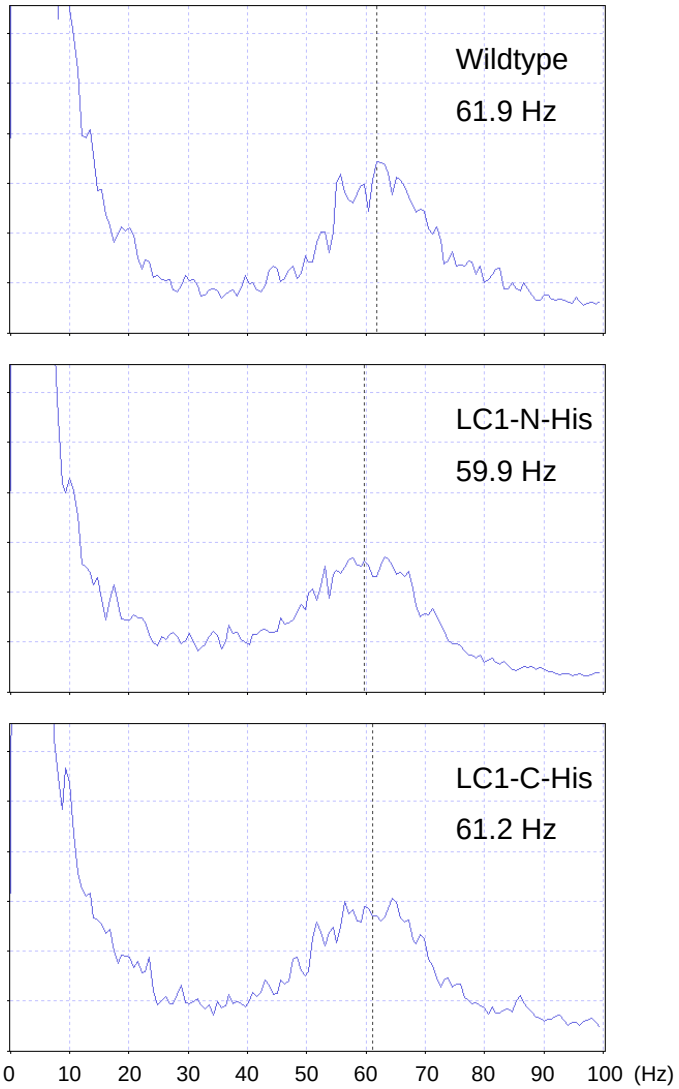
Wildtype
61.9 Hz
LC1-N-His
59.9 Hz
LC1-C-His
61.2 Hz
0
10
20
30
40
50
60
70
80
90
100
(Hz)

B

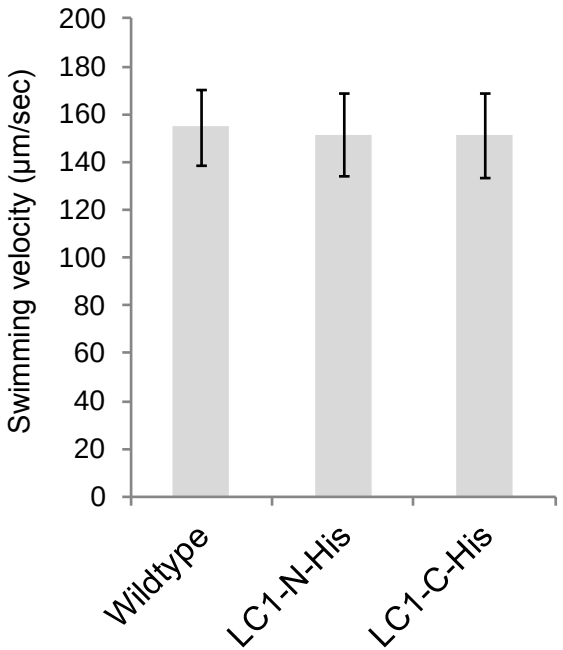
Swimming velocity (μm/sec)
200
180
160
140
120
100
80
60
40
20
0
Wildtype
LC1-N-His
LC1-C-His

Fig S2

A

LC1-C-hsGFP

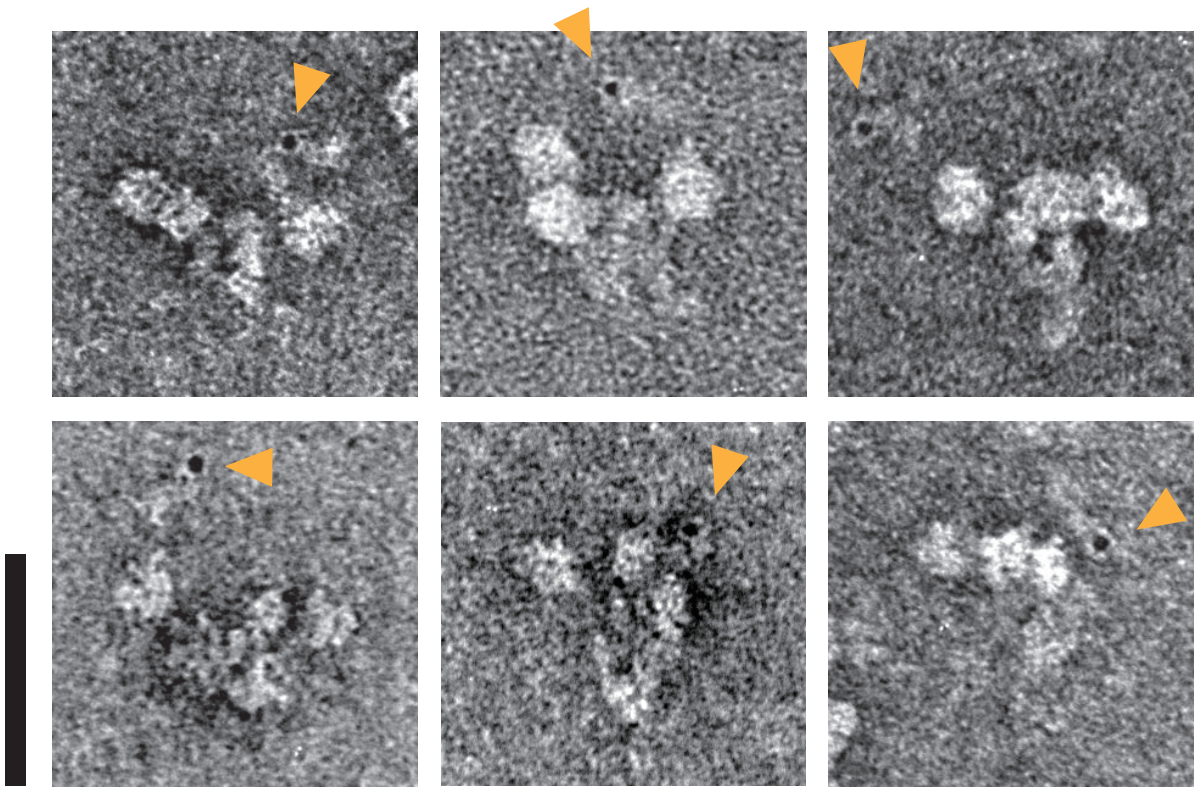

B

βHC-C-hGFP

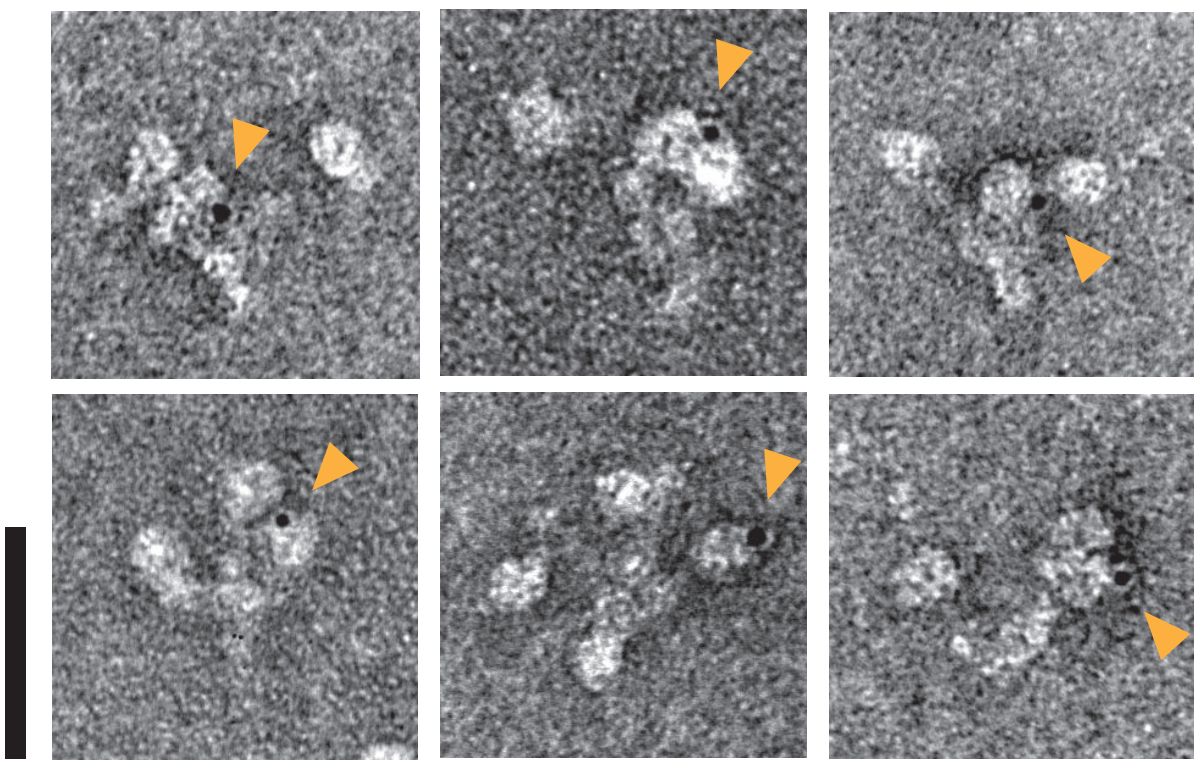

Fig S3

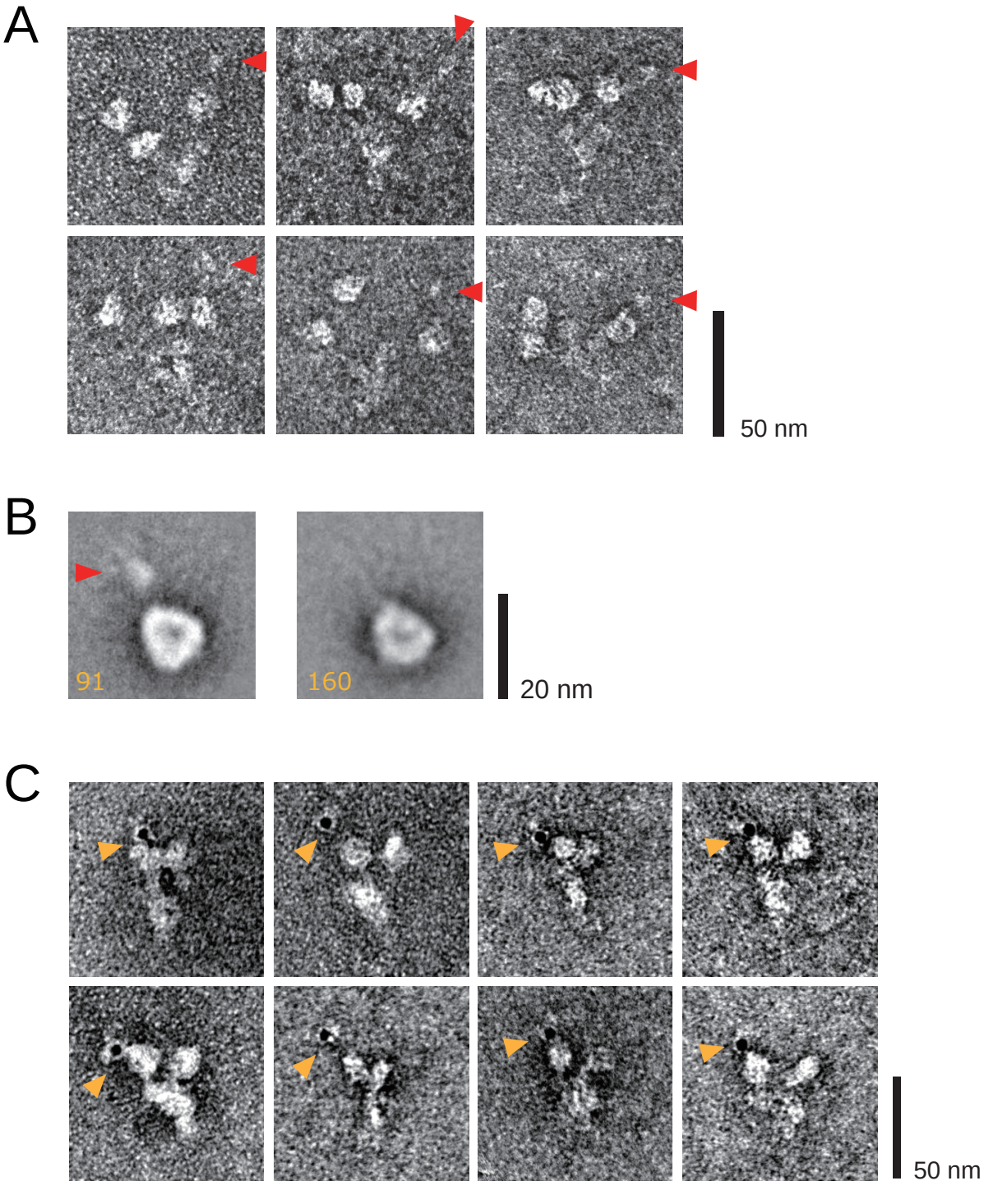

Fig S4

A

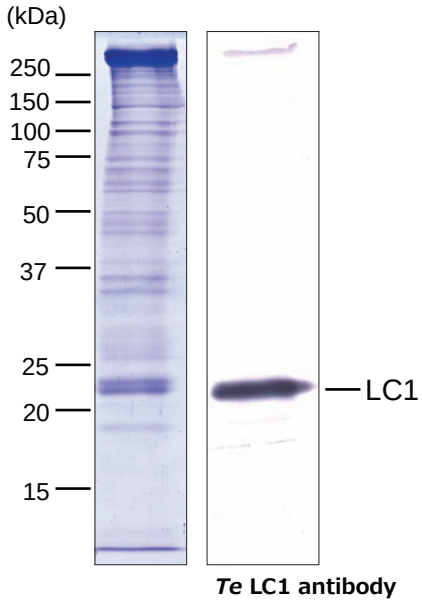
(kDa)
250
150
100
75
50
37
25
20
15
LC1
Te LC1 antibody

B

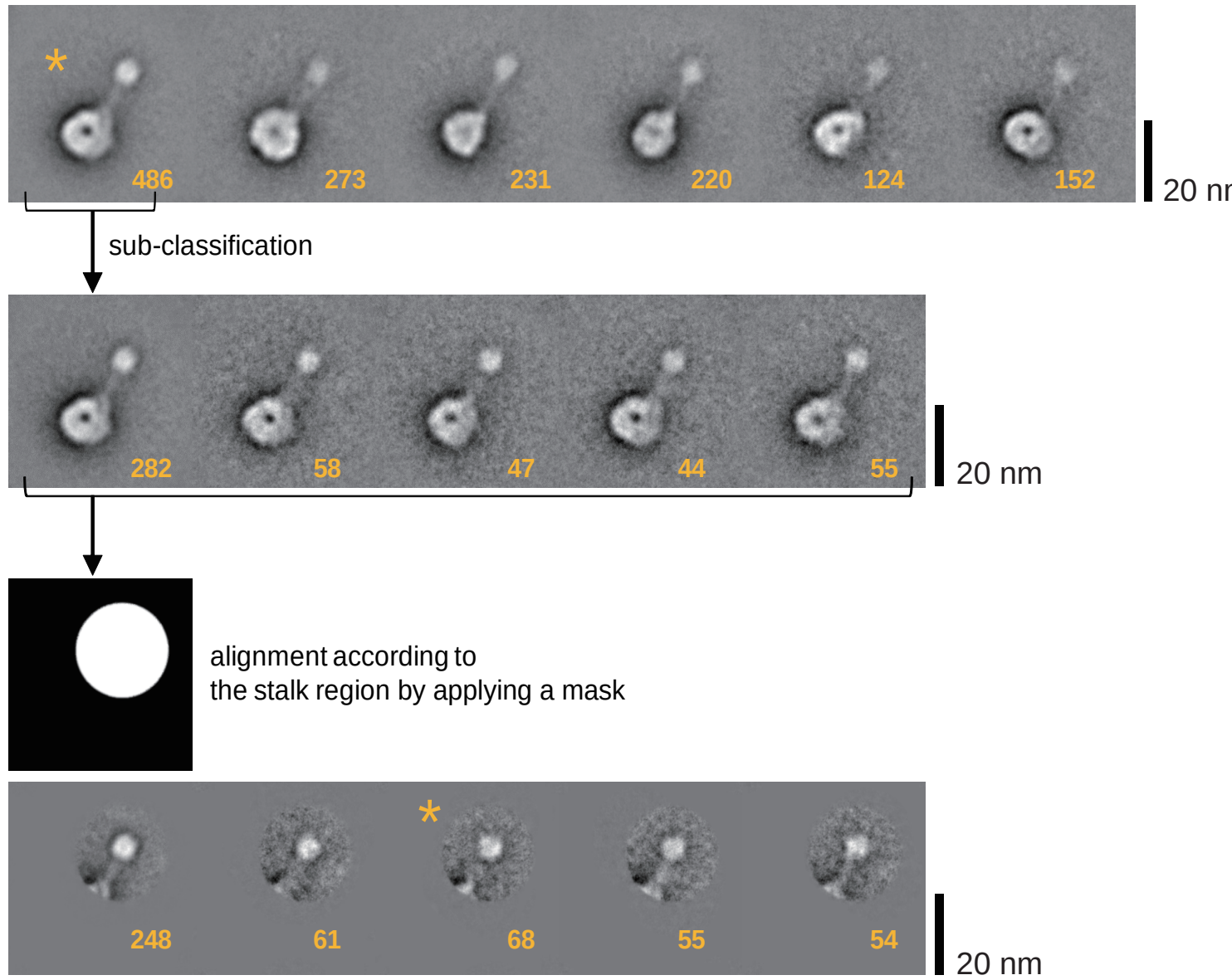
*
486
273
231
220
124
152
20 nm
sub-classification
282
58
47
44
55
20 nm
alignment according to
the stalk region by applying a mask
*
248
61
68
55
54
20 nm

C

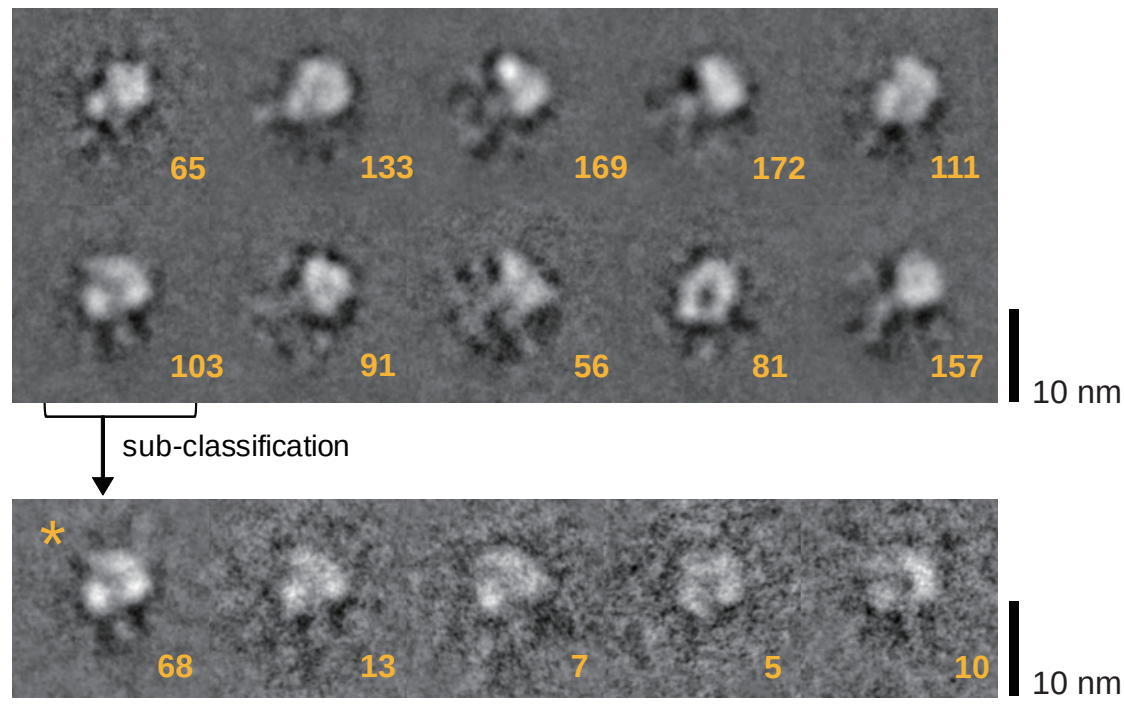
65
133
169
172
111
103
91
56
81
157
10 nm
sub-classification
*
68
13
7
5
10
10 nm

Fig S5

A

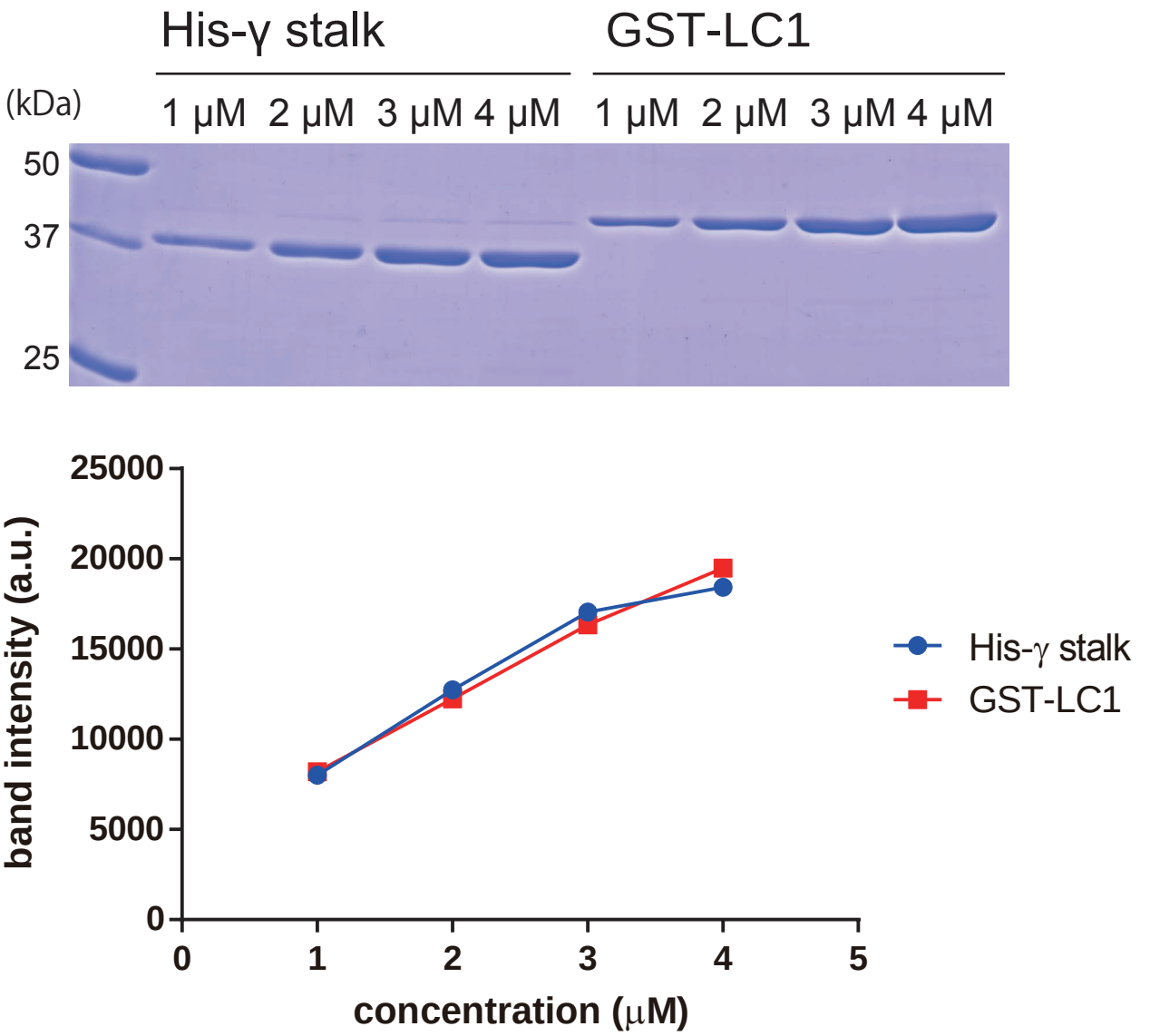
His-γ stalk
GST-LC1
(kDa)
1 μM 2 μM 3 μM 4 μM
1 μM 2 μM 3 μM 4 μM
50
37
25
band intensity (a.u.)
25000
20000
15000
10000
5000
0
0
1
2
3
4
5
concentration (μM)
His-γ stalk
GST-LC1

B

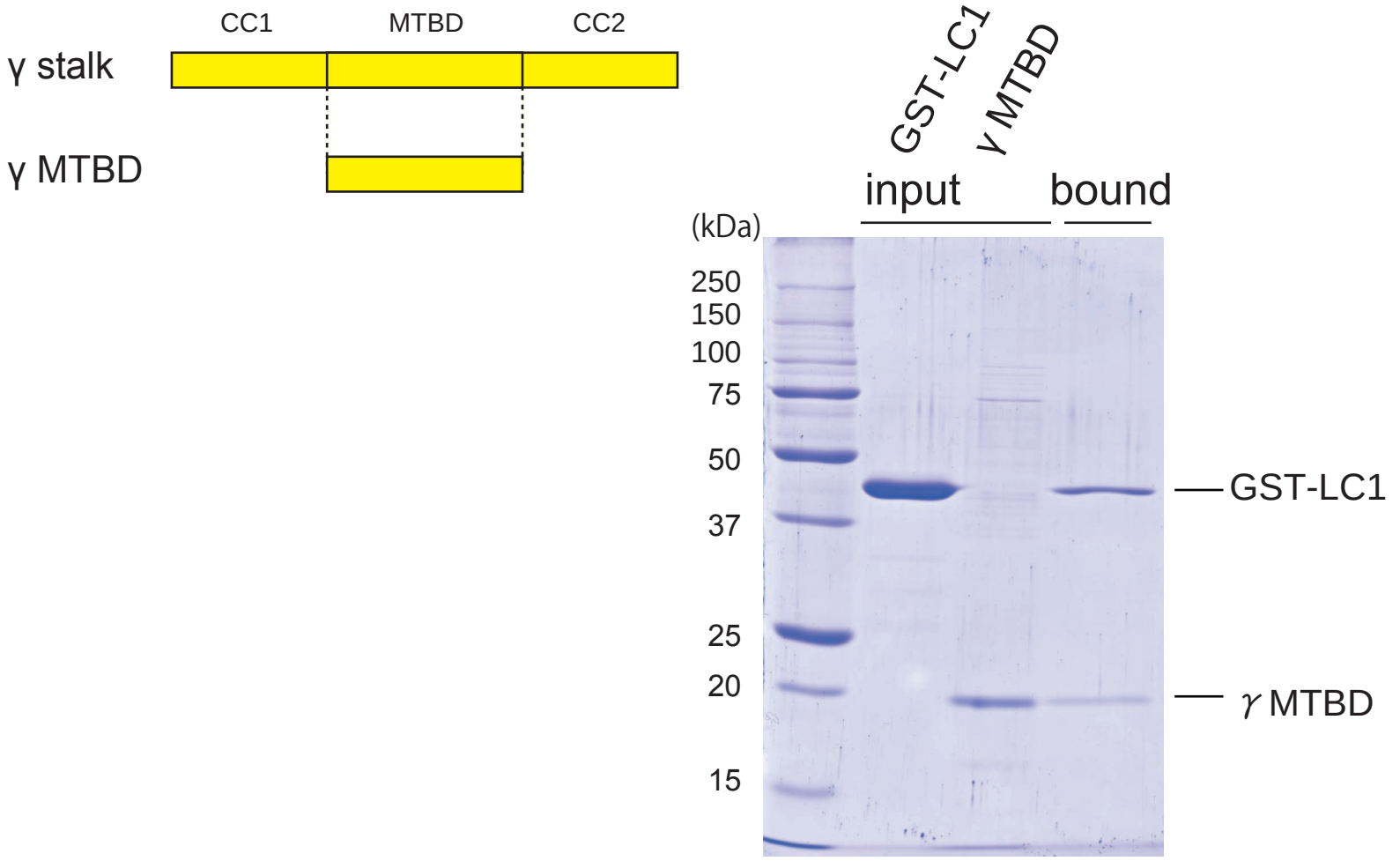
CC1
MTBD
CC2
γ stalk
γ MTBD
GST-LC1
γ MTBD
input
bound
(kDa)
250
150
100
75
50
37
25
20
15
GST-LC1
γ MTBD

Fig S6

A

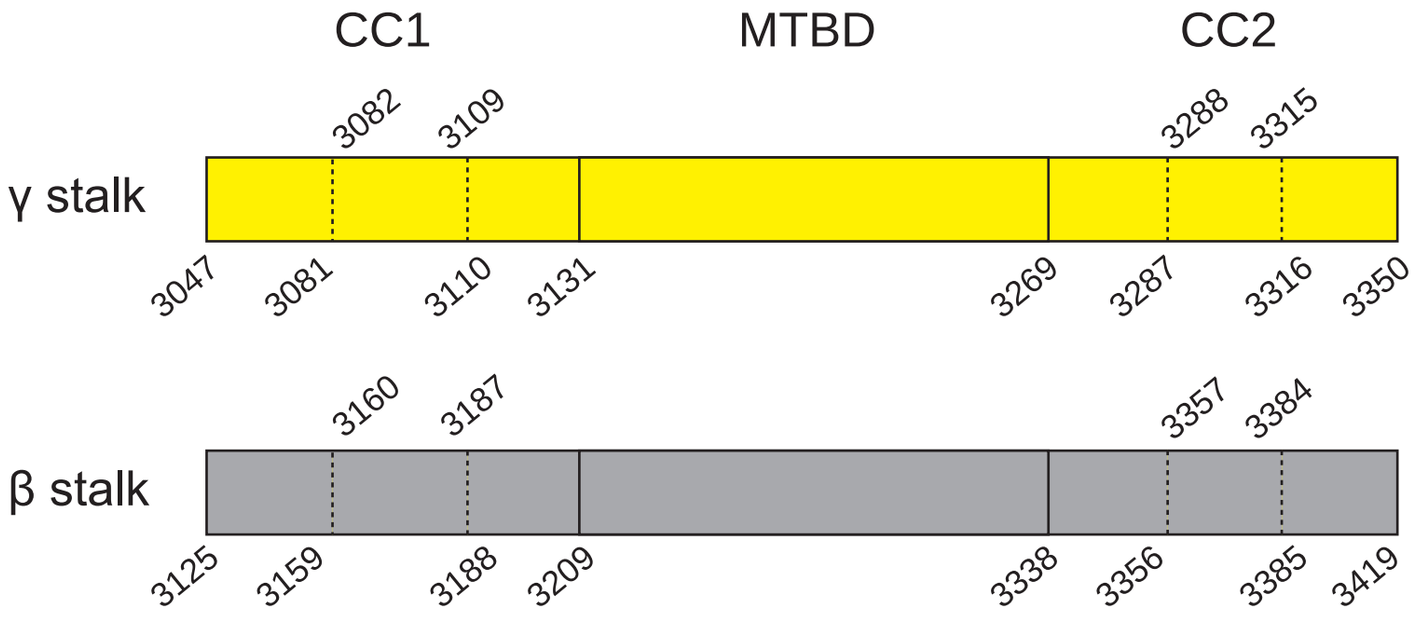
CC1
MTBD
CC2
γ stalk
β stalk
3082
3109
3288
3315
3047
3081
3110
3131
3269
3287
3316
3350
3160
3187
3357
3384
3125
3159
3188
3209
3338
3356
3385
3419

B

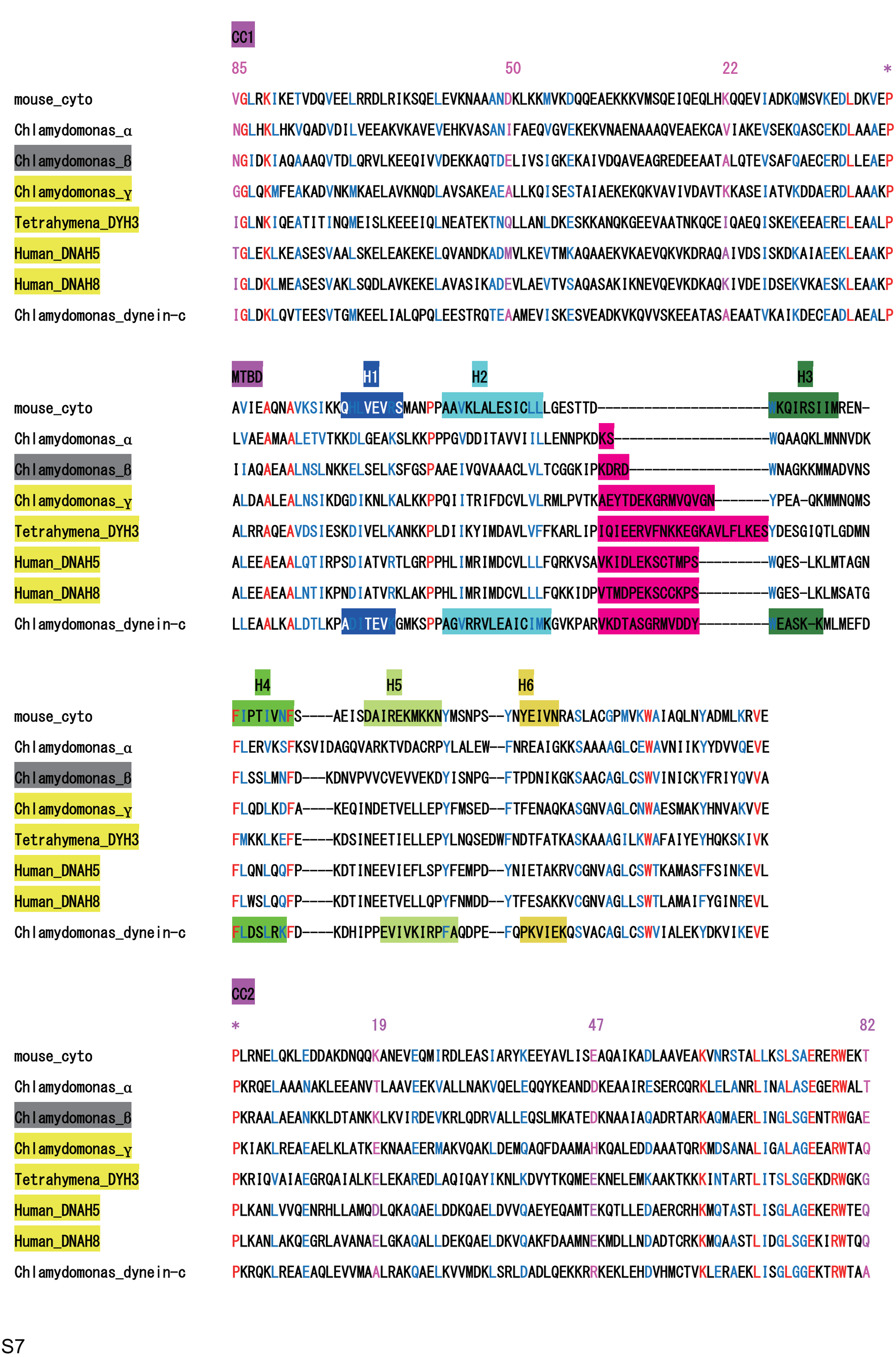
CC1
85 50 22 *
mouse_cyto VGLRKIKETVDQVEELRRDLRIKSQELEVKNAAANDKLKKMVKDQQEAEKKKVMSQEIQEQLHKQQEVIADKQMSVKEDLDKVEP
Chlamydomonas_α NGLHKLHKVQADVDILVEEAKVKAVEVEHKVASANIFAEQVGVEKEKVNAENAAAQVEAEKCAVIAKEVSEKQASCEKDLAAAEP
Chlamydomonas_β NGIDKIAQAAAQVTDLQRVLKEEQIVVDEKKAQTDELIVSIGKEKAIVDQAVEAGREDEEAATALQTEVSAFQAECERDLLEAEP
Chlamydomonas_γ GGLQKMFEAKADVNKMKAELAVKNQDLAVSAKEAEALLKQISESTAIAEKEKQKVAVIVDAVTKKASEIATVKDDAERDLAAAKP
Tetrahymena_DYH3 IGLNKIQEATITINQMEISLKEEEIQLNEATEKTNQLLANLDKESKKANQKGEEVAATNKQCEIQAEQISKEKEEAERELEAALP
Human_DNAH5 TGLEKLKEASESVAALSKELEAKEKELQVANDKADMVLKEVTMKAQAAEKVKAEVQKVKDRAQAIVDSISKDKAIAEEKLEAAKP
Human_DNAH8 IGLDKLMEASESVAKLSQDLAVKEKELAVASIKADEVLAEVTVSAQASAKIKNEVQEVKDKAQKIVDEIDSEKVKAESKLEAAKP
Chlamydomonas_dynein-c IGLDKLQVTEESVTGMKEELIALQPQLEESTRQTEAAMEVISKESVEADKVKQVVSKEEATASAEAATVKAIKDECEADLAEALP
MTBD H1 H2 H3
mouse_cyto AVIEAQNAVKSIKKQHLVEVRSMANPPAAVKLALESICLLLGESTTD----------WKQIRSIIMREN-
Chlamydomonas_α LVAEAMAALETVTKKDLGEAKSLKKPPPGVDDITAVVIILLENNPKDKS----------WQAAQKLMNNVDK
Chlamydomonas_β IIAQAEAALNSLNKKELSELKSFGSPAAEIVQVAAACLVLTCGGKIPKDRD----------WNAGKKMMADVNS
Chlamydomonas_γ ALDAALEALNSIKDGDIKNLKALKKPPQIITRIFDCVLVLRMLPVTKAEYTDEKGRMVQVGN-------YPEA-QKMMNQMS
Tetrahymena_DYH3 ALRRAQEAVDSIESKDIVELKANKKPLDIIKYIMDAVLVFFKARLIPIQIEERVFNKKEGKAVLFLKESYDESGIQTLGDMN
Human_DNAH5 ALEEAEAALQTIRPSDIATVRTLGRPPHLIMRIMDCVLLLFQRKVSAVKIDLEKSCTMPS---------WQES-LKLMTAGN
Human_DNAH8 ALEEAEAALNTIKPNDIATVRKLAKPPHLIMRIMDCVLLLFQKKIDPVTMDPEKSCCKPS---------WGES-LKLMSATG
Chlamydomonas_dynein-c LLEAALKALDTLKPADITEVKGMKSPPAGVRRVLEAICIMKGVKPARVKDTASGRMVDDY---------WEASK-KMLMEFD
H4 H5 H6
mouse_cyto FIPTIVNFS----AEISDAIREKMKKNYMSNPS--YNYEIVNRASLACGPMVKWAIAQLNYADMLKRVE
Chlamydomonas_α FLERVKSFKSVIDAGQVARKTVDACRPYLALEW--FNREAIGKKSAAAAGLCEWAVNIIKYYDVVQEVE
Chlamydomonas_β FLSSLMNFD---KDNVPVVCVEVVEKDYISNPG--FTPDNIKGKSAACAGLCSWVINICKYFRIYQVVA
Chlamydomonas_γ FLQDLKDFA----KEQINDETVELLEPYFMSED--FTFENAQKASGNVAGLCNWAESMAKYHNVAKVVE
Tetrahymena_DYH3 FMKKLKEFE----KDSINEETIELLEPYLNQSEDWFNDTFATKASKAAAGILKWAFAIYEYHQKSKIVK
Human_DNAH5 FLQNLQQFP----KDTINEEVIEFLSPYFEMPD--YNIETAKRVCGNVAGLCSWTKAMASFFSINKEVL
Human_DNAH8 FLWSLQQFP----KDTINEETVELLQPYFNMDD--YTFESAKKVCGNVAGLLSWTLAMAIFYGINREVL
Chlamydomonas_dynein-c FLDSLRKFD----KDHIPPEVIVKIRPFAQDPE--FQPKVIEKQSVACAGLCSWVIALEKYDKVIKEVE
CC2
* 19 47 82
mouse_cyto PLRNELQKLEDDAKDNQQKANEVEQMIRDLEASIARYKEEYAVLISEAQAIKADLAAVEAKVNRSTALLKSLSAERERWEKT
Chlamydomonas_α PKRQELAAANAKLEEANVTLAAVEEKVALLNAKVQELEQQYKEANDDKEAAIRESERCQRKLELANRLINALASEGERWALT
Chlamydomonas_β PKRAALAEANKKLDTANKKLKVIRDEVKRLQDRVALLEQSLMKATEDKNAAIAQADRTARKAQMAERLINGLSGENTRWGAE
Chlamydomonas_γ PKIAKLREAEAELKLATKEKNAAEERMAKVQAKLDEMQAQFDAAMAHKQALEDDAAATQRKMDSANALIGALAGEEARWTAQ
Tetrahymena_DYH3 PKRIQVAIAEGRQAIALKELEKAREDLAQIQAYIKNLKDVYTKQMEEKNELEMKAAKTKKKINTARTLITSLSGEKDRWGKG
Human_DNAH5 PLKANLVVQENRHLLAMQDLQKAQAELDDKQAELDVVQAEYEQAMTEKQTLLEDAERCRHKMQTASTLISGLAGEKERWTEQ
Human_DNAH8 PLKANLAKQEGRLAVANAELGKAQALLDEKQAELDKVQAKFDAAMNEKMDLLNDADTCRKKMQAASTLIDGLSGEKIRWTQQ
Chlamydomonas_dynein-c PKRQKLREAEAQLEVVMAALRAKQAELKVVMDKLSRLDADLQEKKRRKEKLEHDVHMCTVKLERAEKLISGLGGEKTRWTAA

Fig S7

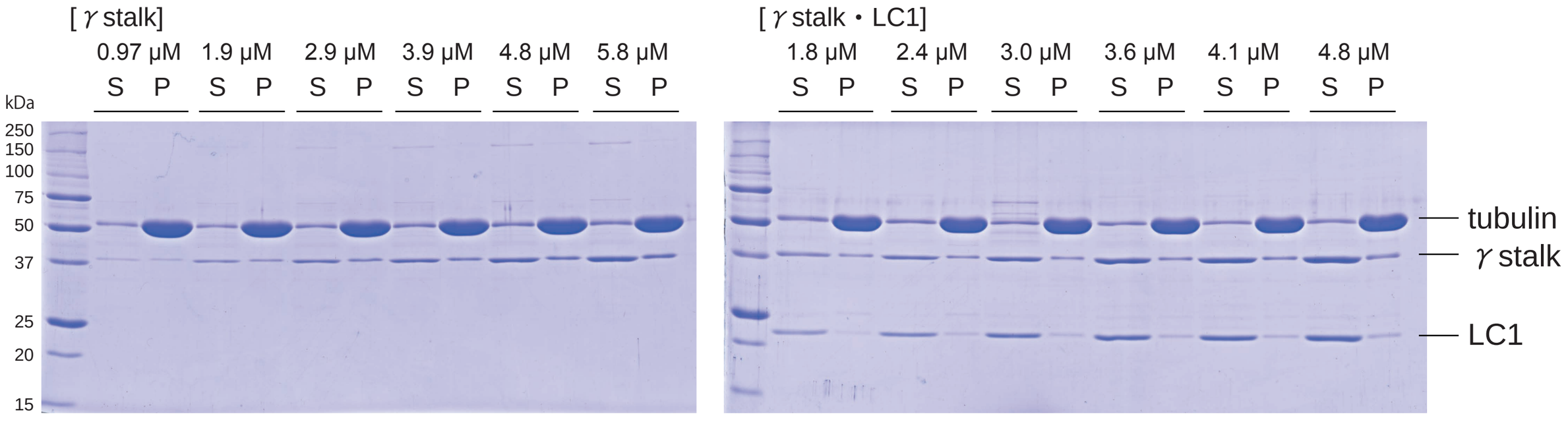

S: supernatant
P: precipitate

Fig S8

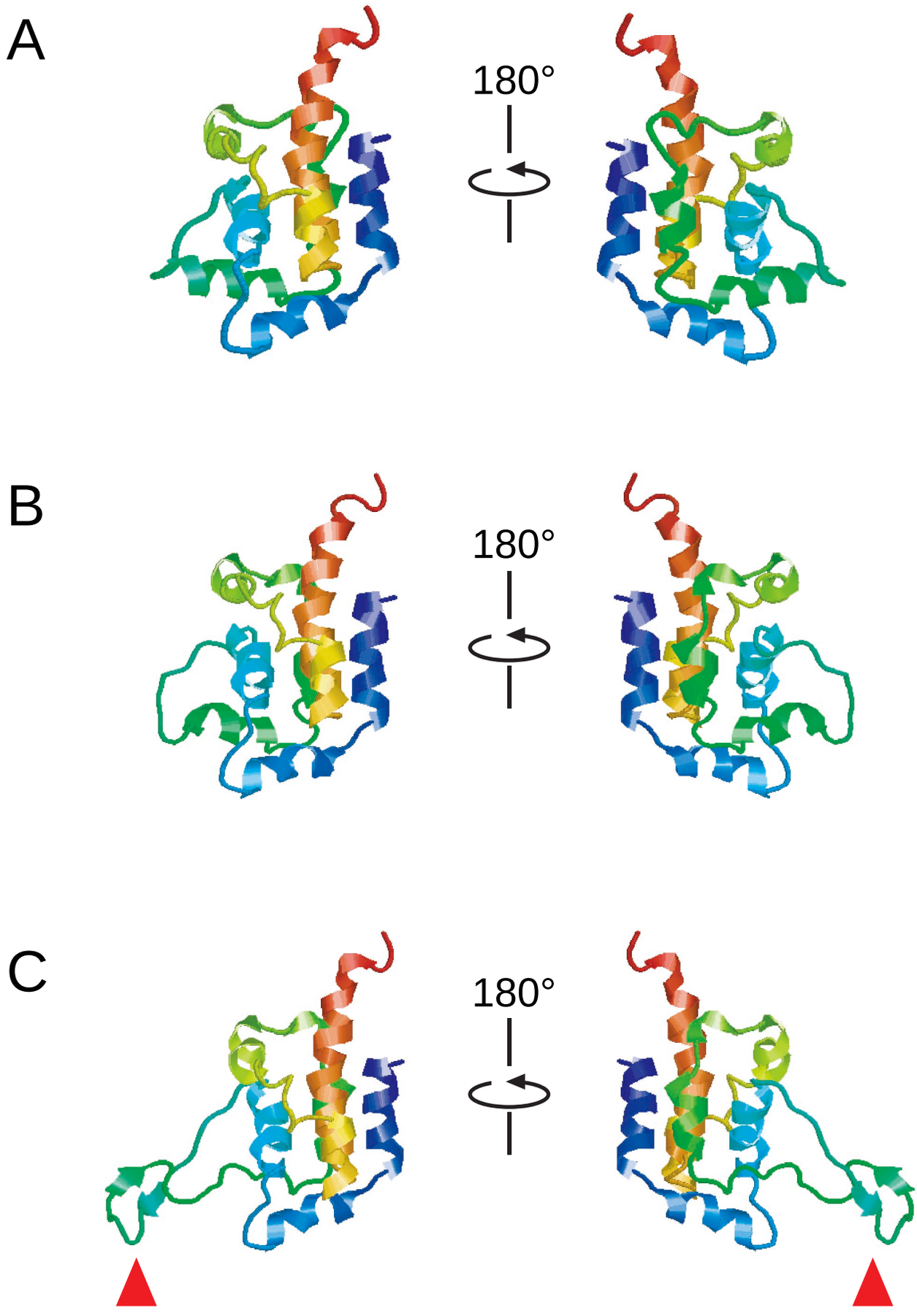

Fig S9

Table S1. Summary of the primers used in this study

purpose	primer name	sequence
Chlamydomonas tagging	LC1-5p-F	5'-CAATCTCAGTTTCACCGCATCAAC
	LC1-3p-R	5'-TGGAGCACAAATTTTGAGGAATGA
	LC1-N-8xHis-1	5'-CCCACCACCACCACCACCACCACCACGGCG
	LC1-N-8xHis-2	5'-CGCCGTGGTGGTGGTGGTGGTGGTGGGG
	LC1-F1	5'-AGACAAGCCCCCAACACCAA
	LC1-C-8xHis-SpeI-R	5'-CGCACTAGTGGTGGTGGTGGTGGTGGTGTCCTCCGCGGGCCACGTT
	LC1-3p-XbaI-F	5'-CGCTCTAGACACCGCTAGCTTTGGGCA
Tetrahymena tagging		
phGFP-neo4 construction	phGFP-inverse-F	5'-CATCATCATCATGGTTCTGGTGGTTCAGTTCAATTAGCTGAT
	phGFP-inverse-R	5'-ATGATGATGATGACCAGAACCATCTTCAATATTATGTCTAATTTTA
phsGFP-neo4 constrcution	phsGFP-inverse-1st-F	5'-CCTTAAGGTTAAAGAGAACCTTCTCATGGTTCTGGTTCAGTTCAATTAGCTGATCATT
	phsGFP-inverse-1st-R	5'-ACCTCTCCAACCAGTAGTCTTTTCATCCATAGAACCATGATGATGATGATGATGAT
	phsGFP-inverse-2nd-F	5'-TAGAATAATTAAGAGCTAGATTAGAACATCATCCTTAAGGTTAAAGAGAACCTTCTC
	phsGFP-inverse-2nd-R	5'-ATTCACCAGCTAAACCTTCAACAACATGACCACCTCTCCAACCAGTAGTCTTTTCA
hGFP-neo4, hsGFP-neo4-fragment	GFP-neo4-F	5'-GGTGGTATGGTTTCTAAGGGTGAAGAACTTTTCACTGGTGTTGTT
	GFP-neo4-R	5'-AAGCTTGATATCGAATTCAGATCCCCCGGGCTGCATTTTTCCAGT
LC1	LC1-C-F	5'-GCTGATGGCGATGAATGAACACTGTATTTTACCAGTCAATCAATCTGATAGAA
	LC1-C-R	5'-AAGTTCTTCACCCTTAGAAACCATACCACCAAGTTATTTAGCTGAAATAGGGATATCTG
	LC1-3'-F	5'-CCCGGGGGATCTGAATTCGATATCAAGCTTTATGTTTTCCATCTATGCGATAAATTATGC
	LC1-3'-R	5'-GCGAGCACAGAATTAATACGACTGGTGGAGAAGGCGACAATTAA
βHC	βHC-C-F	5'-GCTGATGGCGATGAATGAACACTGGGTTTCCGTACAGACTAATGTAA
	βHC-C-R	5'-AAGTTCTTCACCCTTAGAAACCATACCACCCTTTTTATCTTTCTTAACTTCATCAGAGAC
	βHC-3'-F	5'-CCCGGGGGATCTGAATTCGATATCAAGCTTGAAAAATCATAAAAAATTTAAAATAATAAACATTTCTATA
	βHC-3'-R	5'-GCGAGCACAGAATTAATACGACTTCCTGATAAACCTTCAGAATAAGG
overlapping PCR	overlap-outer-F	5'-GCTGATGGCGATGAATGAACACTG
	overlap-outer-R	5'-GCGAGCACAGAATTAATACGACT
PCR check	βHC-genome-check-R	5'-CAACTAAGACATATAAACAGCAAGG
	LC1-genome-check-R	5'-TCGTCAAATCATAGCATAATTTATCGC
Construction for biochemical experiments		
αstalk	OADα-85:82-XhoISalI-F	5'-GAACTCGAGGTCGAC AACGGCCTGCACAAGCTGCAC
	OADα-85:82-HindIII-R	5'-CTGAAGCTTCGTCAGCGCCCAGCGC
βstalk	OADβ-85:82-XhoISalI-F	5'-GAACTCGAGGTCGACAACGGTATTGACAAGATTGCACAGGC
	OADβ-85:82-HindIII-R	5'-CTGAAGCTTTTCGGCGCCCCAGCG
γstalk	OADγ-85:82-XhoISalI-F	5'-GAACTCGAGGTCGACGGTGGCCTGCAGAAGATGTTTGAG
	OADγ-85:82-HindIII-R	5'-CTGAAGCTTCTGCGCCGTCCAGCGC
LC1	LC1-BamHI-F	5'-GTGGATCCATGGCCAAGGCAACTAC
	LC1-EcoRI-R	5'-CAGAATTCCTATCCTCCGCGGGC
Chimeric stalk constructs		
β35:35-γ50:47	β35:35-inverse-F	5'-AAGAACGCCGCCATCGCGCA
	β35:35-inverse-R	5'-GTCGGTCTGCGCCTTCTTCT
	γ50:47-F	5'-GCGCTGCTGAAGCAGATTAG
	γ50:47-R	5'-GTGCGCCATGGCGGCATCGA
β63:63-γ22:19	β63:63-inverse-F	5'-CTGAAGGTCATTCGTGACGA
	β63:63-inverse-R	5'-GGTGGCCGCCTCCTCATCCT
	γ22:19-F	5'-AAGAAGGCCAGCGAGATTGC
	γ22:19-R	5'-CTCCTTGGTGGCCAGCTTGA
β85:82-γMTBD	β85:82-inverse-F	5'-AAGCGTGCGGCCCTGGCAGA
	β85:82-inverse-R	5'-CTCAGCCTCCAGCAGGTCGC
	γMTBD-F	5'-CCCGCGCTGGATGCTGCCCT
	γMTBD-R	5'-GGGCTCCACCACCTTGGCCA
γ35:35-β50:47	γ35:35-inverse-F	5'-AAGCAGGCGCTGGAGGACGA
	γ35:35-inverse-R	5'-CTCCGCCTCCTTGGCCGACA
	β50:47-F	5'-GAGCTGATTGTGTCCATCGG
	β50:47-R	5'-GTCCTCCGTAGCCTTCATGA
γ63:63-β22:19	γ63:63-inverse-F	5'-AAGAACGCCGCCGAGGAGCG
	γ63:63-inverse-R	5'-CGTCACGGCGTCCACAATCA
	β22:19-F	5'-GCGCTGCAGACTGAGGTGTC
	β22:19-R	5'-CTTCTTGTTGGCGGTGTCCA
γ85:82-βMTBD	γ85:82-inverse-F	5'-AAGATTGCCAAGCTGCGCGA
	γ85:82-inverse-R	5'-CTTGGCGGCAGCCAGGTCGC
	βMTBD-F	5'-CCCATCATTGCGCAGGCCGA
	βMTBD-R	5'-GGGCGCCACCACCTGGTAGA
Construction of γMTBD fragment	OADγ-MTBD-XhoI-F	5'-CCGCTCGAGCCCGCGCTGGATGCTGCCCT
	OADγ-MTBD-HindIII-R	5'-CCCAAGCTTGGGCTCCACCACCTTGGCCA

Figure S1. Recombinant *Chlamydomonas* and *Tetrahymena*, and recombinant OAD complex.

(A) Assessment of His-tagged *Chlamydomonas* LC1.

(i) Western blots of axonemes of WT and LC1-N-His recombinant strains by *Chlamydomonas* LC1 antibody (*Ch* LC1 antibody).

(ii) Western blots of the OAD complexes of WT and LC1-C-His by *Chlamydomonas* LC1 antibody (*Ch* LC1 antibody). The OAD complex in (ii) was prepared by the ATP extraction. Both His-tagged and wild-type LC1 were detected in (i) and (ii).

(iii) The OAD complex was extracted from recombinant *Chlamydomonas* axonemes under high salt conditions and further affinity purified using a Ni-NTA affinity.

(B) Assessment of *Tetrahymena* transformants.

(i) PCR was performed using genomic DNA purified from the WT strain or transformants (strains βHC-C-hGFP and LC1-C-hsGFP) using primer sets βHC-C-F/βHC-genome-check-R or LC1-C-F/LC1-genome-check-R. The positions of the primer annealing sites are shown in the schematic diagram. By phenotypic assortment process, the wild type genes were replaced by recombinant genes. For the βHC-C-hGFP strain, single cell lines were obtained (strains-1, 2, and 3). All ~45 copies of genes in strain-3 were thought to be replaced by recombinant genes because no wild-type genes were detected in cells cultured without paromomycin (unlike for the strains-1 and 2).

(ii) Both the recombinant β HC and LC1 were detected in *Tetrahymena* cilia by GFP fluorescence. Arrowheads indicate the oral apparatus. Bar, 20 μm.

(C) Assessment of the recombinant *Tetrahymena* OAD constructs.

(i) βHC-C-hGFP was detected in cilia by Western blots using anti *Tetrahymena* β HC antibody (*Te* βHC antibody) and anti GFP antibody. The βHC-C-hGFP protein was purified using Ni-NTA resin.

(ii) LC1-C-hsGFP was detected in cilia and in the OAD complex by Western blots using anti GFP antibody and anti *Tetrahymena* LC1 antibody (*Te* LC1 antibody). The LC1-C-hsGFP OAD complex was extracted in high salt condition and further purified by SBP-tag on the LC1.

Figure S2. Characterization of motility of recombinant *Chlamydomonas*.

The beat frequencies (A) and swimming velocities (B) of wild type and the recombinant *Chlamydomonas*. The mean values for swimming velocities are as follows: Wild type, 154.8 ± 15.8 μm/sec; LC1-N-His, 151.4 ± 17.4 μm/sec; LC1-C-His, 151.5 ± 17.8 μm/sec (mean ± SD, n = 20 each).

Figure S3. EM images of *Tetrahymena* OAD complex.

(A) Schematic diagram of the LC1-C-hsGFP construct and EM images of the Ni-NTA-nanogold labeled *Tetrahymena* LC1-C-hsGFP OAD complex. Gold particles (orange arrowheads) bound at one of the stalk tips. Note that the distribution of the gold particles was wider than in the labeling of the *Chlamydomonas* LC1 (Figure 1A), possibly because of the flexibility of the hsGFP-tag.

(B) Ni-NTA-nanogold labeling of the *Tetrahymena* βHC-C-hGFP OAD complex.

The gold particles (orange arrowheads) were found at the edge of the AAA+ ring. Scale bars, 50 nm.

Figure S4. Supplemental results for the large stalk tip.

(A) EM images of the native *Tetrahymena* OAD complex.

(B) Class averages of the head domains of *oda11 Chlamydomonas* OAD.

Representative class averages with (left side) or without (right side) extra density (red arrowhead) are shown. The numbers of EM images are shown.

(C) Ni-NTA-nanogold labeling of *oda11*×LC1-C-His *Chlamydomonas* OAD.

One of the stalk tips in the βγ two-headed structure was labeled with Ni-NTA-nanogold (orange arrowheads).

Figure S5. Data related to the single particle analysis of *Tetrahymena* DYH3 head fragment.

(A) SDS-PAGE and Western blots of purified *Tetrahymena* DYH3 head fragment.

The main band at the top of the gel represents the DYH3 head fragment. The minor bands are thought to correspond to degradation products due to chymotryptic digestion. The purified DYH3 head fragment was found to associate with endogenous LC1 by Western blots using *Tetrahymena* LC1 antibody (*Te* LC1 antibody).

(B) Single particle analysis of *Tetrahymena* DYH3 head and stalk region.

Class averages of *Tetrahymena* DYH3 head fragments showing the large stalk tip (top row). Similar EM images in the major group (indicated by orange asterisk) were sub-classified into five classes by K-means clustering (middle row). Subsequently, the images were aligned according to the stalk region by applying a mask shown (bottom row). The mask was applied to most of the AAA+ ring except the base of the stalk, so that information on the stalk angle was retained. Orange asterisks denote the class averages shown in Figure 3, and the numbers of images are indicated.

(C) Single particle analysis of the stalk-tip region.

Class averages of the stalk-tip region are shown in the upper two rows. In some classes, the large stalk tip image was composed of two sub-structures. One class average was sub-classified and the representative class average is shown in Figure 3B-iii (orange asterisk). The numbers of images are shown.

Figure S6. Supplemental results for Figure 4.

(A) Relationship between molar concentration and band intensities.

Known concentration of His-γ stalk and GST-LC1 (1-4 μM, 11.25 μl each) were assessed by SDS-PAGE and the band intensities were measured using ImageJ (NIH). Mean value of the band intensity ratios (His-γ stalk /GST-LC1) was 1.0, therefore, band intensity ratio (His-γ stalk/GST-LC1) can be considered as molar ratio. Co-purified His-γ stalk and GST-LC1 in Figure 3C-(i) is within this range.

(B) GST pull-down assay using γ MTBD region fragment.

Schematic diagram of γ MTBD region fragment sequence and result of GST pull-down assay. γ MTBD fragment was detected in bound fraction together with GST-LC1. Here, GST pull-down assay was performed basically same as in Figure 5, except that concentration of γ MTBD fragment was 450 nM.

Figure S7. Comparison of the stalk sequences.

(A) Schematic diagrams of the γ (yellow) and β (gray) stalk region sequences. The numbers of the amino acid residues used as junction sites for the chimeric stalk constructs are shown.

(B) Amino acid sequence of the stalk region of mouse cytoplasmic dynein HC, *Chlamydomonas* α, β and γ HCs, *Tetrahymena* DYH3 HC, human DNAH5 HC, human DNAH9 HC, and *Chlamydomonas* inner arm dynein-c. The regions corresponding to amino acids 3,047-3,350 of the *Chlamydomonas* γ HC were aligned (identical residues, red; similar residues, blue). The *Chlamydomonas* γ HC and its homologues are indicated in yellow, and *Chlamydomonas* β HC is indicated in gray. The MTBD is defined as the region between two highly conserved proline residues (magenta asterisks). The numbers of amino acid residues in CC1 and CC2, counted from the proline residues, are shown above. Residues shown in magenta were used for the junction sites for the chimeric constructs. Known structural information of the MTBD, helix 1-6 (H1-H6), is highlighted, based on Carter *et al*. (2008) and Kato *et al*. (2014). The insert sequences between H2 and H3 are highlighted in magenta.

Figure S8. SDS-PAGE images of the microtubule co-pelleting assay.

SDS-PAGE results of the microtubule co-pelleting assay of γ stalk, γ stalk-LC1 complex, and LC1. Fixed concentration of microtubule (5 μM) was incubated with increasing concentrations of γ stalk (0.97-5.8 μM), γ stalk-LC1 complex (1.8-4.8 μM), and LC1 (1.0-6.3 μM). After centrifugation, the supernatant fraction and precipitation fraction were analyzed by SDS-PAGE. The images of gels were digitized and the intensities of the bands were quantified.

Figure S9. Homology models of the MTBD region.

Homology models were built from the NMR structure of dynein-c MTBD (PDB: 2RR7) for α HC (A), β HC (B), and γ HC (C). Only the γ MTBD was predicted to have the "flap" structure (red arrowheads). Note that the flap structure alone cannot explain the size of the additional structure in Figure 3B.

Supplemental materials and methods

Strains and culture conditions

Chlamydomonas reinhardtii strains used were WT (137C), *oda11* (Sakakibara et al., 1991), *oda4-s7* (Sakakibara et al., 1993), LC1-N-His, LC1-C-His, LC2-C-His (Furuta et al., 2009) and *oda11*×LC1-C-His. Cells were grown in liquid Tris-acetate-phosphate medium (Gorman and Levine, 1965) with aeration on a 12 h light and 12 h dark cycle, or on solid medium containing 1.5% agar.

Tetrahymena thermophila strains used were WT SB255, WT B2086, βHC-C-hGFP, and LC1-C-hsGFP. Cells were cultivated in SPP media (1% proteose peptone No.3, 0.2% glucose, 0.1% yeast extract, 0.003% Fe-EDTA) or in PYD media (1% proteose peptone No.3, 0.87% glucose, 0.5% yeast extract). Appropriate concentration of Cd^{2+} and paromomycin for selection were added to the media if necessary.

Antibodies

To generate antibodies against *Chlamydomonas* LC1's 104-198 aa region, the cDNA sequence coding this region was amplified by PCR from wild type cDNA and subcloned into the pCold proS2 DNA vector (Takara) between *Nde*I and *BamH*I sites. In brief, the plasmid was transformed into *E. coli* BL21-CodonPlus (DE3) RIL (Stratagene) and induced protein was purified using the His-tag. After the His-tag and proS2-tag were removed by Thrombin digestion (Sigma), the relevant peptide fragment was separated by SDS-PAGE and used as the antigen to generate rabbit polyclonal antibody. For the production of antibody against *Tetrahymena* LC1, a peptide fragment corresponding to the 131-144 aa region (NWEELDKLKDLPEL) was synthesized as the antigen to generate rabbit polyclonal antibody.

Purification of *Chlamydomonas* OAD complex

Isolation and demembranation of *Chlamydomonas* flagella were performed by standard methods (Witman et al., 1986). *Chlamydomonas* OAD complexes were extracted from the axonemes either by high salt extraction (0.6 M KCl, 30 mM HEPES pH 7.4, 1 mM EGTA, 5 mM $MgSO_4$) or ATP extraction (5 mM ATP, 75 mM PIPES pH 6.8, 1 mM $MgCl_2$, 1 mM EGTA, 1 mM GTP, 1 mM DTT, 10 μg/ml leupeptin, 1 mM PMSF, 10 μM paclitaxel) (Goodenough and Heuser, 1984). The extracted OAD complex was further fractionated by 10-40% (w/v) sucrose density gradient centrifugation in 0.1 mM ATP, 75 mM PIPES pH 6.8, 1 mM $MgCl_2$, 1 mM EGTA, 1 mM GTP, 1 mM DTT, 10 μg/ml leupeptin, 1 mM PMSF and 10 μM paclitaxel. For EM observation, the OAD complex purified by ATP extraction was used, since the three-headed structure was more readily observed in this condition.

Purification of *Tetrahymena* OAD complex

Tetrahymena cells were deciliated by the addition of 2 mM Ca^{2+} (Rosenbaum and Carlson, 1969). Demembranation of cilia was performed by adding 0.1% NP-40. *Tetrahymena* OAD complexes were isolated from the axoneme by high salt extraction (0.6 M NaCl, 10 mM HEPES-NaOH pH7.4, 4 mM $MgSO_4$, 5 mM EGTA, 0.1 mM PMSF). The extracted recombinant OAD complex containing LC1-C-hsGFP was purified by SBP-tag using Strep-Tactin Sepharose resin (IBA), according to Ichikawa et al. (2011). Recombinant OAD complex containing βHC-C-hGFP was purified by His-tag using Profinity IMAC Ni-Charged Resin (Bio-Rad), and imidazole was removed from eluted protein with a NAP5 column (GE Healthcare). Purification of the wild-type OAD complex and chymotryptic

digestion to obtain the DYH3 head fragment was performed as in Yamaguchi et al. (2015).

Tagging of *Chlamydomonas* LC1

To make *Chlamydomonas* LC1 expression constructs, a ~3.8 kb fragment containing the LC1 gene was amplified from wild-type *Chlamydomonas* genomic DNA using primers LC1-5p-F and LC1-3p-R. Primers used in this study are shown in Table S1. The PCR product was cloned into the *Eco*RV site of pBluescript II (Agilent Technologies) to create the construct pLC1. For N-terminal tagging with 8 × His, two oligo nucleotides, LC1-N-8×His-1 and LC1-N-8×His-2, were annealed and inserted into the *Msc*I site of pLC1 to create the construct pLC1-N-His. For C-terminal tagging with 8 × His, two LC1 genomic fragments were amplified using primer sets LC1-F1/LC1-C-8×His-SpeI-R and LC1-3p-XbaI-F/LC1-3p-R. The two amplification products were digested with *Spe*I and *Xba*I, ligated together, and the product was digested with *Nco*I and *Aat*II and used to replace the untagged LC1 gene in pLC1 to create pLC1-C-His. Each of the two His-tagged LC1 plasmids was linearized with *Eco*RI and co-transformed with pSI103 (PMID: 11602359) into wild-type *Chlamydomonas* cells by electroporation. Cells expressing His-tagged LC1 were screened by Western blots. A cross between the LC1-C-His strain and strain *oda11* was produced using standard methods (Harris, 1989).

Tagging of *Tetrahymena* OAD subunits.

pEGFP-neo4 vector (Kataoka et al., 2010) was modified so that an 8 × His-tag was introduced in a loop region of EGFP as in Kobayashi et al. (2008) by inverse PCR using primer set phGFP-inverse-F and phGFP-inverse-R (phGFP-neo4 vector). The phGFP-neo4 vector was further modified so as to carry an SBP-tag by inverse PCR using primer sets phsGFP-inverse-1st-F/phsGFP-inverse-1st-R and phsGFP-inverse-2nd-F/phsGFP-inverse-2nd-R (phsGFP-neo4 vector). Homologous recombination into the *Tetrahymena* macronucleus was performed as in Kataoka et al. (2010). In brief, an hsGFP-neo4-fragment was amplified from phsGFP-neo4 vector with primers GFP-neo4-F and GFP-neo4-R. The DNA sequences encoding the C-terminal region of LC1 (LC1-C-fragment; 1,263 bp) and the 3' flanking region (LC1-3'-fragment; 1,475 bp) were amplified from *Tetrahymena* genomic DNA with primer sets LC1-C-F/LC1-C-R and LC1-3'-F/LC1-3'-R. These three fragments were integrated by overlapping PCR using primers overlap-outer-F and overlap-outer-R. Transformation was performed using a PDS-1000/He biolistic delivery system (BioRad). To select transformants, a drug resistance gene was induced with 1 μg/ml Cd^{2+}, and 100 μg/ml paromomycin was added for selection. hGFP-tagging to *Tetrahymena* βHC was performed similarly. Since the *Tetrahymena* macronucleus holds ~45 copies of genes, a phenotypic assortment process was performed to obtain transformants with a high copy number of the recombinant gene (Wood et al., 2007). The concentration of Cd^{2+} was reduced gradually to 0.01 μg/ml, and then the paromomycin concentration was increased gradually to 850 μg/ml for the LC1-C-hsGFP strain and 600 μg/ml for the βHC-C-hGFP strain. The increase of the ratio of recombinant genes was assessed by GFP fluorescence and PCR analysis (Supplemental Figure S1B). For the βHC-C-hGFP strain, a single cell line whose β HC genes were completely replaced with recombinant genes was obtained and used for the study (strain-3 in Supplemental Figure S1B). GFP fluorescence images were acquired using a CCD camera (iXonEM DV860, Andor) attached to an IX70 microscope (Olympus) equipped with a confocal scanner unit (CSU10, Yokogawa).

180

181 **Measurements of swimming velocity and beat frequency.**

182 Swimming of *Chlamydomonas* was recorded using BX53 microscope (Olympus) equipped with a CCD
183 camera (ADT-33S, FLOVEL). Swimming velocities of *Chlamydomonas* cells were analyzed using
184 ImageJ MTrack2 plug-in (http://valelab.ucsf.edu/~nstuurman/ijplugins/MTrack2.html). Beat
185 frequencies of *Chlamydomonas* cells were measured by fast Fourier transform (FFT) analysis of
186 vibrations of the cells (Kamiya, 2000).

187

188 **Construction of proteins for biochemical experiments.**

189 The cDNA regions encoding the stalk regions of α, β and γ HC were amplified from *Chlamydomonas* cDNA with
190 appropriate primer pairs (Supplemental Table S1) so that the numbers of amino acid residues in CC1 and CC2 would
191 be 85 and 82 respectively. The fragments were subcloned into pColdI vector between *Xho*I and *Hind*III sites, and
192 pColdI-α stalk, pColdI-β stalk and pColdI-γ stalk were obtained. pColdI-γ MTBD was constructed similary. The
193 cDNA region coding *Chlamydomonas* LC1 was amplified and inserted into vector pGEX-6P-2 between *Bam*HI and
194 *Eco*RI sites to produce pGEX-6P-2-LC1. To create chimeric stalk constructs with a β HC base and a γ HC tip (β35:35-
195 γ50:47, β63:63-γ22:19, β85:82-γMTBD), pColdI-β stalk vector was linearized by inverse PCR and fragments
196 encoding the γ stalk-tip region or the γ MTBD region were amplified from pColdI-γ stalk by PCR. These fragments
197 were integrated by blunt-end ligation and pColdI-β35:35-γ50:47, pColdI-β63:63-γ22:19 and pColdI-β85:82-γMTBD
198 vectors were obtained. pColdI-β35:35-γ50:47, pColdI-β63:63-γ22:19 and pColdI-β85:82-γMTBD vectors were
199 created vice versa. All PCR products were verified by sequencing.

200

201 **Purification of proteins for biochemical experiments.**

202 The resultant plasmids were transformed into *E. coli* BL21-CodonPlus (DE3) RIL. Cells were cultured in 500 ml LB
203 medium supplemented with 50 μg/ml ampicillin at 37°C until the optical density OD_{600} reached 0.4-0.5. For
204 constructs in pColdI, cells were cultured for a further 24 h after the temperature was lowered to 15°C and 0.1 mM
205 isopropyl-1-thio-β-D-galactopyranoside (IPTG) was added to the media for induction. Cells containing pGEX-6P-2-
206 LC1 were cultured for a further 3 h at 20°C after 0.4 mM IPTG was added. For the stalk constructs and γ MTBD
207 fragment, purification was performed using the His-tag derived from the pColdI vector. The cells were lysed with
208 His-tag lysis buffer (50 mM Tris-HCl pH 8.0, 150 mM NaCl, 20 mM imidazole), sonicated, and ultracentrifuged.
209 The supernatant obtained was left to bind to Profinity IMAC Ni-Charged Resin (BIO-RAD) for 30 min, 4°C. The
210 resin was washed three times with His-tag wash buffer (50 mM Tris-HCl pH 8.0, 250 mM NaCl, 20 mM imidazole)
211 and bound protein was eluted with His-tag elution buffer (50 mM Tris-HCl pH 8.0, 150 mM NaCl, 300 mM
212 imidazole). LC1 construct was purified using the GST-tag from vector pGEX-6P-2. For the purification of GST-
213 tagged LC1 (GST-LC1), the cell pellet was resuspended, sonicated, and ultracentrifuged in PBS (10 mM Na_2HPO_4,
214 1.8 mM KH_2PO_4, 140 mM NaCl, 2.7 mM KCl, pH 7.3) containing 1 mM DTT. GST•Bind Resin was added to the
215 supernatant and incubated for 60 min at 4°C. The resin was washed three times with PBS containing 1 mM DTT. To
216 obtain GST-tagged LC1 (GST-LC1), protein was eluted with GST elution buffer (50 mM Tris-HCl pH8.0, 100 mM
217 NaCl, 10 mM glutathione). To purify LC1 without a GST-tag, PreScission base buffer (50 mM Tris-HCl pH 7.5, 150

mM NaCl, 1 mM EDTA) was used instead of PBS, and the GST-tag was removed by incubating with PreScission base buffer containing 1 mM DTT and PreScission protease (GE Healthcare) overnight at 4°C. To perform tandem affinity purification of His-γstalk and GST-LC1, the supernatants of *E.coli* expressing either His-γ stalk or GST-LC1 were mixed for 1 h at 4°C prior to sequential purification using the His-tag and the GST-tag. For all the purified proteins, buffer was exchanged to NAP5 buffer by using NAP5 columns (GE Healthcare). Protein concentrations were determined according to Read and Northcote (1981) using BSA as the standard.

Computational analysis

To quantify band intensities, ImageJ (NIH) or Quantity One software (BioRad) were used. Data analysis was performed using Excel, Sigmaplot and GraphPad Prism 6. Statistical analyses were performed using GraphPad Prism 6. Alignment of sequences was performed by Clustal W (Thompson et al., 1994). For homology modeling of the MTBD structure, Swiss Model Server (Arnold et al., 2006) was used.

References

Arnold, K., Bordoli, L., Kopp, J., & Schwede, T. (2006). The SWISS-MODEL workspace: a web-based environment for protein structure homology modelling. *Bioinformatics*, *22*(2), 195-201.

Gorman, D. S., & Levine, R. P. (1965). Cytochrome f and plastocyanin: their sequence in the photosynthetic electron transport chain of Chlamydomonas reinhardi. *Proceedings of the National Academy of Sciences of the United States of America*, 54(6), 1665.

Harris, E. H. (1989). The chlamydomonas sourcebook (Vol. 2). San Diego: Academic Press.

Ichikawa, M., Watanabe, Y., Murayama, T., & Toyoshima, Y. Y. (2011). Recombinant human cytoplasmic dynein heavy chain 1 and 2: observation of dynein-2 motor activity in vitro. *FEBS letters*, 585(15), 2419-2423.

Kamiya, R. (2000). Analysis of cell vibration for assessing axonemal motility in Chlamydomonas. Methods. 22:383–387. http://dx.doi.org/10.1006/ meth.2000.1090

Kataoka, K., Schoeberl, U. E., & Mochizuki, K. (2010). Modules for C-terminal epitope tagging of *Tetrahymena* genes. *Journal of Microbiological Methods*, *82*(3), 342-346.

Read, S. M., & Northcote, D. H. (1981). Minimization of variation in the response to different proteins of the Coomassie blue G dye-binding assay for protein. *Analytical biochemistry*, 116(1), 53-64.

Rosenbaum, J. L., & Carlson, K. (1969). Cilia regeneration in Tetrahymena and its inhibition by colchicine. *The Journal of Cell Biology*, 40(2), 415-425.

Sakakibara, H., Mitchell, D. R., & Kamiya, R. (1991). A Chlamydomonas outer arm dynein mutant missing the alpha heavy chain. *The Journal of Cell Biology*,113(3), 615-622.

Sakakibara, H., Takada, S., King, S. M., Witman, G. B., & Kamiya, R. (1993). A Chlamydomonas outer arm dynein mutant with a truncated beta heavy chain. *Journal of Cell Biology*, 122(3), 653-661.

Thompson, J. D., Higgins, D. G., & Gibson, T. J. (1994). CLUSTAL W: improving the sensitivity of progressive multiple sequence alignment through sequence weighting, position-specific gap penalties and weight matrix choice. *Nucleic Acids Research*, *22*(22), 4673-4680.

Witman, G. B. (1986). Isolation of Chlamydomonas flagella and flagellar axonemes. *Methods in enzymology*, 134, 280-290.

Wood, C. R., Hard, R., & Hennessey, T. M. (2007). Targeted gene disruption of dynein heavy chain 7 of Tetrahymena thermophila results in altered ciliary waveform and reduced swim speed. *Journal of Cell Science*, 120(17), 3075-3085.